

Contents lists available at ScienceDirect

# **Chemical Physics Letters**

journal homepage: www.elsevier.com/locate/cplett





# Raman spectroscopic, computational, and X-ray crystallographic investigation of intermolecular interactions in trimethylamine *N*-oxide (TMAO) and TMAO-d<sub>9</sub>

Louis E. McNamara <sup>a</sup>, Ethan C. Lambert <sup>a</sup>, Dana N. Reinemann <sup>b</sup>, Henry Valle <sup>c</sup>, T. Keith Hollis <sup>c</sup>, Gregory S. Tschumper <sup>a</sup>, Nathan I. Hammer <sup>a</sup>, \*

- <sup>a</sup> Department of Chemistry and Biochemistry, University of Mississippi, University, MS 38677, United States
- <sup>b</sup> Department of Biomedical Engineering, University of Mississippi, University, MS 38677, United States
- <sup>c</sup> Department of Chemistry, Mississippi State University, Mississippi State, MS 39762, United States

#### ARTICLE INFO

Keywords: TMAO Raman spectroscopy Density functional theory Intermolecular interactions

#### ABSTRACT

Crystalline structures of trimethylamine N-oxide (TMAO) and its isomorphic, perdeuterated analogue (TMAO-d<sub>9</sub>) were investigated using Raman spectroscopy, X-ray crystallography, and electronic structure theory. Shifts to higher vibrational energy were observed in both Raman Under liquid Nitrogen Spectroscopy (RUNS) and high pressure Raman spectroscopy studies. Agreement between experimental Raman spectra and electronic structure computations performed on individual TMAO molecules was poor; however, better agreement was obtained when model unit cells were considered. These results also show that TMAO-d<sub>9</sub>'s spectra are significantly less perturbed than those for TMAO, suggesting weaker interactions between neighboring TMAO molecules when deuterated.

# 1. Introduction

Trimethylamine *N*-oxide (TMAO) belongs to a family of naturally occurring 'counteracting' osmolytes [1] which are known to help maintain cell volume under osmotic and hydrostatic stress, stabilize the native structure of proteins, and counteract the destabilizing effect of denaturants [2–7]. Work performed by Somero et al. in the late 1970s through early 1980s suggests osmolyte concentrations are a result of convergent evolution to survive environmental stress while retaining the functionality of biological macromolecules [1,8]. Even though a number of previous reports have shown that TMAO stabilizes proteins [9,10], the precise molecular mechanism has not been firmly established in the literature [2,6,11–29]. The molecular structure of TMAO suggests two main types of biologically relevant intermolecular interactions: the oxygen atom can act as a hydrogen bond acceptor and its three methyl groups can also participate in hydrophobic interactions.

There has been extensive research by our groups and others into the impact of aqueous TMAO on the local hydrogen bonding networks of water and other similar solvents [24,29–31]. However, there is very little literature exploring the chemical properties of interacting TMAO

molecules, aggregation of TMAO, and TMAO in the crystalline phase and how these interactions may impact its behavior in solution. This lack of emphasis seems to be largely a result of TMAO's biological relevance overshadowing its importance as a benchmark system for strong dipole—dipole interactions. Crystalline TMAO is a desirable system for study not only for its prospect as a prototypical high dipole moment molecule but also because of TMAO's inherent biological significance.

Here, we investigate the crystal structures of TMAO and TMAO-d<sub>9</sub> as well as elucidate the effects of temperature and pressure on the vibrational structure of both systems using Raman spectroscopy under pressure in a diamond anvil cell, under liquid nitrogen using Raman Under liquid Nitrogen Spectroscopy (RUNS), and with electronic structure theory. The substitution of hydrogen by deuterium has served as a powerful tool to investigate the vibrational and spin dependent properties of systems since the discovery of deuterium in 1932 [32]. Since changes in the vibrational structure are easily detectable upon hydrogen/deuterium (H/D) substitution, Raman spectroscopy is an ideal tool to probe the structural effects of deuteration on local noncovalent bonding networks.

<sup>\*</sup> Corresponding author at: Department of Chemistry and Biochemistry, University of Mississippi, P.O. Box 1848, University, Mississippi 38655, United States. E-mail address: nhammer@olemiss.edu (N.I. Hammer).

#### 2. Methods

#### 2.1. Materials

Commercial grade anhydrous trimethylamine N-oxide (98% pure) was purchased from Sigma-Aldrich and perdeuterated d<sub>9</sub>-trimethylamine N-oxide (TMAO-d<sub>9</sub>, 98% pure) from Cambridge Isotope Laboratories. Both chemicals were used without further purification. Nujol® and ruby spheres for pressure calibration were purchased from AlmaxeasyLab.

#### 2.2. Crystal structure

Powder X-ray diffraction experiments were performed using a Bruker Kappa Apex-II diffractometer. Collection of the X-ray data, unit cell refinement and initial data reduction were performed using the Olex<sup>2</sup> software. SADABS-2012/1 (Bruker, 2012) was used for absorption correction. The structure was solved by direct methods using the SHELXS program and refined with SHELXL [33].

#### 2.3. Computational methods

Density functional theory [34,35] (DFT) computations were performed using the Gaussian 09 software package [36]. The B3LYP density functional [37,38] was employed using a Pople style split valence double- $\zeta$  basis set with polarization and diffuse functions, 6–31+G(d,p). A dense numerical integration grid composed of 99 radial shells and 590 angular points per shell was used for all of DFT calculations. The electronic energy was converged to at least  $10^{-9}$  E<sub>h</sub> and initial geometries were obtained from crystallographic data. Identical geometry optimizations were performed for both TMAO and TMAO-d<sub>9</sub> in isolation in addition to four geometry optimizations with neighboring interactions for each polymorph.

Calculations to simulate interactions in crystalline TMAO were performed by first taking an array of TMAO unit cells and choosing a central TMAO molecule. Next, all TMAO molecules except for the central TMAO and its nearest neighbors were removed. This process left a central TMAO molecule surrounded by 10 neighboring molecules (see Supporting Information for these crystals). The resulting structure was optimized through two different approaches. The 'rigid crystal' method (RC), in which all atoms except those contained by the central TMAO molecule were frozen, and the 'non-rigid crystal' (NRC), in which all non-hydrogen atoms except those contained by the central TMAO molecule were frozen. The positions of the respective hydrogen or deuterium atoms for TMAO and TMAO-do were included in the obtained crystalline structure and are available in the Supporting Information. A similar approach has yielded results consistent with second order Møller-Plesset perturbation theory in previous work investigating small vibrational shifts in pyrimidine induced by complexation with water [39,40] and in the investigation of crystalline pyrimidine [41]. Vibrational frequencies were calculated for both isolated molecules as well as their crystalline polymorphs. Spectra were simulated by summing Lorentzians constructed from the calculated harmonic frequencies and normalized Raman optical activities [42].

# 2.4. High pressure Raman spectroscopy

High pressure Raman spectra were obtained through the use of a diamond anvil cell (DAC). Solid TMAO was packed into a 0.24 mm diameter hole in a stainless steel gasket along with a single ruby sphere. Nujol® was used as a pressure transmitting medium to ensure even compression throughout the sample. The pressure was calculated by tracking the shifts in the Ruby's photoluminescence, R1 line [43,44]. Maximum pressures achieved were on the order of 6 GPa. A Nikon Eclipse TE2000-U inverted microscope paired with a Princeton Instruments ProEM 1024 CCD camera were used for signal collection. A

Princeton Instruments Acton SP2500 monochrometer equipped with a 2400 grooves/mm grating was used to achieve spectral resolution of  $0.01~{\rm cm}^{-1}$ . We estimate the maximum error in reproducibility to be less than 2 cm $^{-1}$  in this setup. The 514.5 nm line of a Coherent Innova Ar $^{+}$  ion laser was employed as the Raman excitation source along with two 520 long pass filters to prevent laser transmission through to the CCD camera

#### 2.5. Raman under liquid nitrogen spectroscopy (RUNS) [45-48]

Raman spectra were also taken under liquid nitrogen using a Jobin-Yvon Ramanor HG2-S Raman spectrometer with two 1800 grooves/mm gratings and a thermoelectrically cooled (-30  $^{\circ}$ C) photomultiplier tube as the detector. A scan speed of 2 cm $^{-1}$ /s was employed. The 514.4 nm line of an Ar/Kr $^{+}$ ion laser was utilized as the Raman excitation source. A stainless steel sample holder surrounded by Styrofoam for insulation held the sample in place while covered in liquid nitrogen.

#### 3. Results and discussion

#### 3.1. Crystal structure

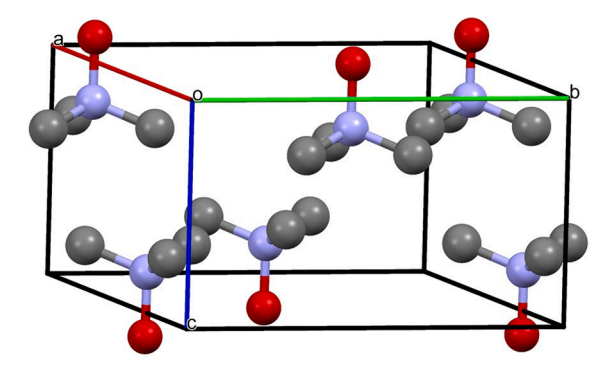
The crystal structure of room temperature TMAO has been previously reported [49]. It belongs to the space group C2/m and its unit cell contains six molecules which are located on mirror planes. The crystal structure of TMAO-d<sub>9</sub> at 220 K was found to be isomorphic with TMAO. Upon cooling the samples to 100 K both TMAO and TMAO-d<sub>9</sub> underwent a phase change to the  $P2_1/c$  space group. This change is accompanied by a reduction in the number of molecules per unit cell from 6 to 4 along with the loss of proper mirror planes and rotation axis. Crystallographic results are summarized in Table 1 and the unit cells for the two space groups are shown in Fig. 1. Each TMAO molecule has 10 neighboring molecules in the first coordination sphere.

#### 3.2. Calculated frequencies

Computed frequencies were scaled by an empirically determined scaling factor of 0.95 for TMAO structures and by 0.965 for TMAO-d to best account for anharmonicity and intermolecular interactions in condensed phases. Detailed below are comparisons of simulated Raman spectra computed using different structural models with experimental spectra acquired under different conditions. Changes in peak ratio are an artifact of the normalization of each wave. For guidance, the following are common frequencies for the vibrations of TMAO and TMAO-d9: the C-N stretching region is found between 750 and 800 cm $^{-1}$ , the N-O stretching region between 930 and 980 cm $^{-1}$  and the symmetric and asymmetric C-H stretching regions are between 2930 and 3070 cm $^{-1}$ ; for TMAO-d9 the C-N/N-O stretching region is found between 675 and

 $\begin{tabular}{ll} \textbf{Table 1} \\ \textbf{Comparison of crystallographic data for TMAO and TMAO-} \textbf{d}_9 \ at \ different temperatures. \end{tabular}$ 

	TMAO[49] 295 K	TMAO 100 K	TMAO-d <sub>9</sub> 220 K	TMAO-d <sub>9</sub> 100 K
Crystal System	monoclinic	monoclinic	monoclinic	monoclinic
Space Group	C2/m	P21/c	C2/m	P21/c
a/Å	10.154	4.9656(2)	10.1326(4)	4.9682(4)
b/Å	8.793	8.5577(3)	8.6194(3)	8.5080(6)
c/Å	5.006	10.0815(4)	4.9956(2)	10.0699(8)
α/deg	90	90	90	90
β/deg	91.03	91.097(2)	91.215(2)	91.321(6)
γ/deg	90	90	90	90
V/Å3	446.884	428.33(3)	436.202(3)	425.54(6)
Z, Z'	4, 0	4, 0	4, 0	4, 0
R-factor (%)	7.9	7.9	3.47	3.44



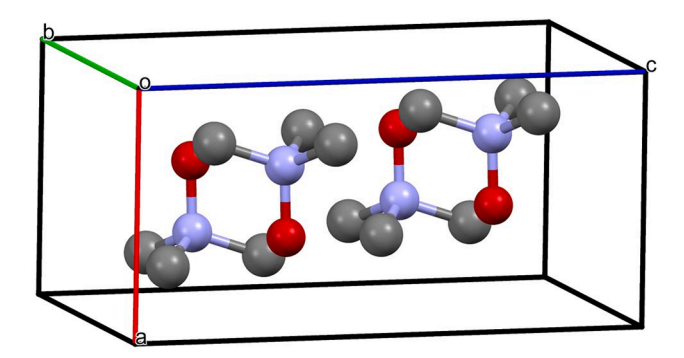


Fig. 1. Unit cells for TMAO in the C2/m (left) and P21/c (bottom) space groups. Hydrogen atoms are omitted for clarity.

 $950~{\rm cm}^{-1}$ , C-D wagging/twisting region between 1025 and 1225 cm $^{-1}$ , and the C-D stretching regions between 2060 and 2340 cm $^{-1}$ .

TMAO - C2/m. Fig. 2 compares experimental and simulated Raman spectra for crystalline TMAO at room temperature. Calculations performed on a single isolated TMAO molecule (SM) results in almost universally poor agreement with experiment in terms of the prominent features in the spectrum. This is expected due to the fact that SM calculations are unable to accurately represent intermolecular interactions in the crystalline phase. The Raman modes in the C-H stretching region are best recovered by the NRC model, suggesting that short contact interactions in the crystal are perturbing the hydrogen atoms and decreasing the degeneracy of the symmetric C-H stretching modes of neighboring TMAO molecules. Both crystal models (RC and NRC) predict a single peak for the N-O stretch (908 cm<sup>-1</sup> both) and C-N-C bend (1242 cm<sup>-1</sup> for RC and 1241 cm<sup>-1</sup> for NRC), in good agreement with experiment. Relative to the SM model, the N-O stretch is significantly blue shifted (increased in energy) by  $\sim 20~{\rm cm}^{-1}$  in both of these models while the C-N-C stretch is relatively unperturbed. This predicts that the N-O stretch should be observed at the same energy as the C-N-C stretch, possibly as a result of the strong dipole–dipole interactions (5.02 D)[23] between the center TMAO molecule and nearest neighbors.

**TMAO - P2**<sub>1</sub>/c. Fig. 3 compares the simulated Raman spectra using the results from calculations of crystalline TMAO in the  $P2_1/c$  space group to experimental RUNS spectra. The agreement between the different methods and the experimental RUNs spectra follows the same trend as observed at room temperature using the C2/m space group. There is little predicted difference between the calculated frequencies of the two models (Fig. 4), with the exception of blue shifts in the C-H stretching region in the NRC model. The RUNS spectra also exhibit in all regions and splitting between the N-O rock and C-N-C bend both around

1280 cm<sup>-1</sup>.

**TMAO-d9** - **C2/m**. In contrast to the all-hydrogen TMAO, the experimental TMAO-d9 spectra show surprisingly good overall agreement with the SM model, especially in the lower fingerprint region. This is shown in Fig. 5. Using the C2/m space group, the C-D stretching region is only accurately predicted by the NRC model. This model, however, drastically overestimates the splitting in the N-O rock and C-N-C bending region. Collectively, these results suggest that intermolecular interactions aren't significantly perturbing the bonds between the heavier atoms but rather are affecting the deuterium atoms.

 $\it TMAO-d_9$  -  $\it P2_1/c$ . Fig. 6 compares the simulated Raman spectra using the results from calculations of crystalline TMAO-d<sub>9</sub> in the  $\it P2_1/c$  space group to the corresponding experimental RUNS spectra. As with the room temperature spectra, the RC model and SM models most accurately predict the lower energy region, while the NRC model most accurately recovers the splitting in the C-H stretching region. Fig. 7 directly compares the experimental room temperature and RUNS spectra for TMAO-d<sub>9</sub>. As in the case of all-hydrogen TMAO, blue shifts relative to the room temperature spectrum in the C-D stretching region are evident and are best predicted by the NRC model.

#### 3.3. High pressure Raman

Figures S1-S2 show the high pressure Raman data obtained using a DAC and peak frequencies are summarized in Fig. 8. The spectra are summarized in several spectral regions in Figures S1 - S2, which roughly correlated to the above mentioned spectral regions. This axial scaling should be considered when qualitatively analyzing blue shifts of the pressurized spectra relative to atmospheric pressure. The Raman vibrational spectra were measured as a function of the total pressure in

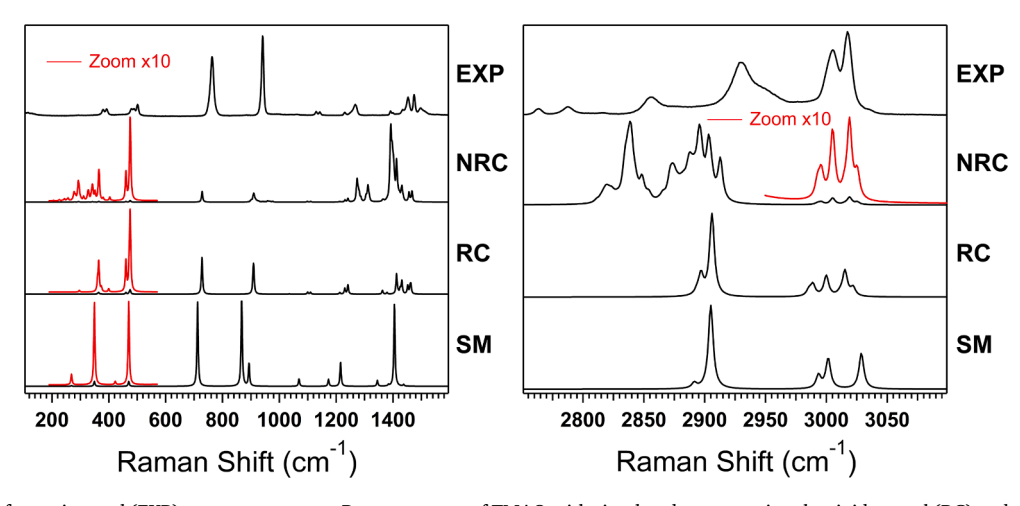


Fig. 2. Comparison of experimental (EXP) room temperature Raman spectra of TMAO with simulated spectra using the rigid crystal (RC) and non-rigid crystal (NRC) models and the C2/m space group, as well as a single isolated molecule (SM).

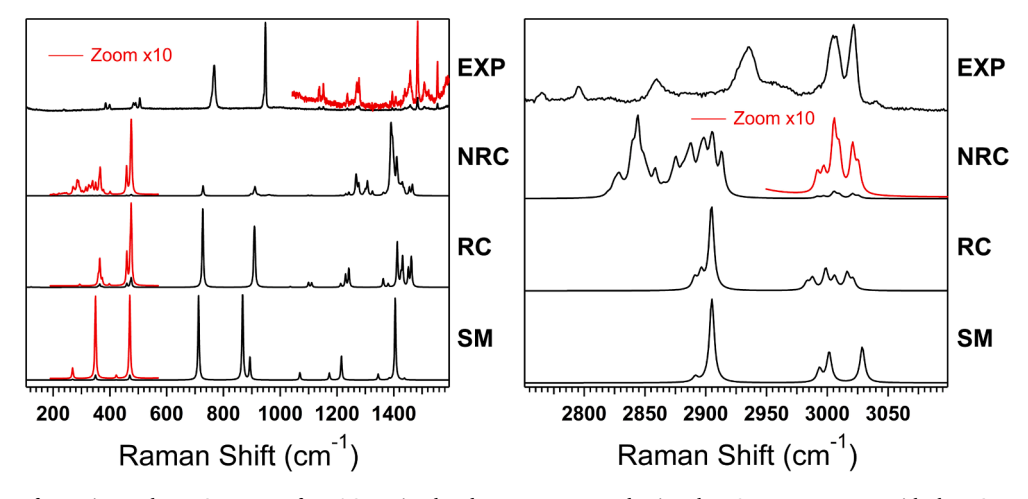


Fig. 3. Comparison of experimental RUNS spectra of TMAO to simulated spectra computed using the P21/c space group with the RC, NRC, and SM models.

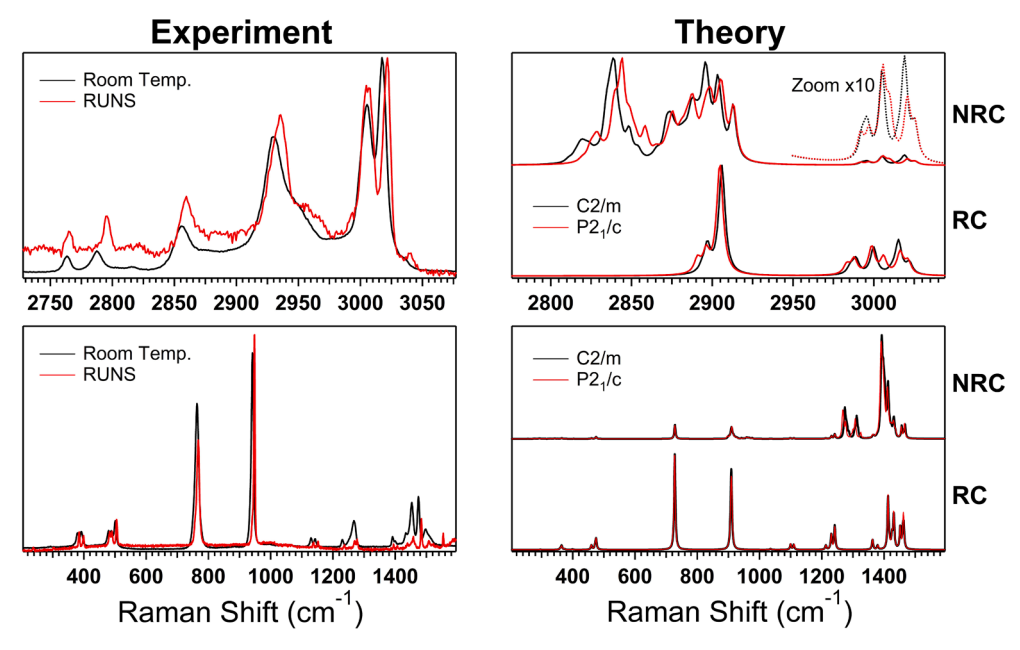


Fig. 4. Comparison of room temperature and RUNS spectra (left) and RC and NRC computational models using the C2/m and  $P2_1/c$  space groups (right) for all-hydrogen TMAO.

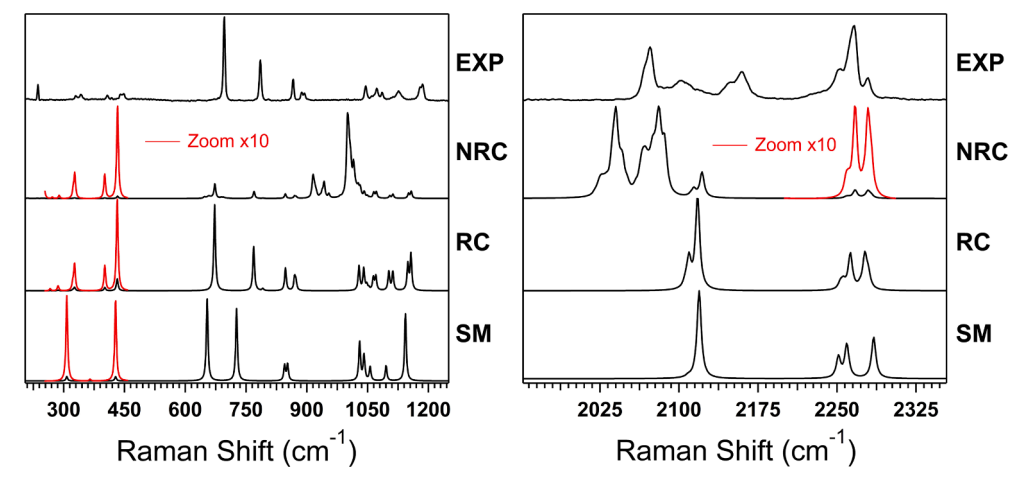


Fig. 5. Comparison of experimental room temperature Raman spectra of TMAO- $d_9$  to calculated spectra using the C2/m space group and the RC, NRC, and SM models.

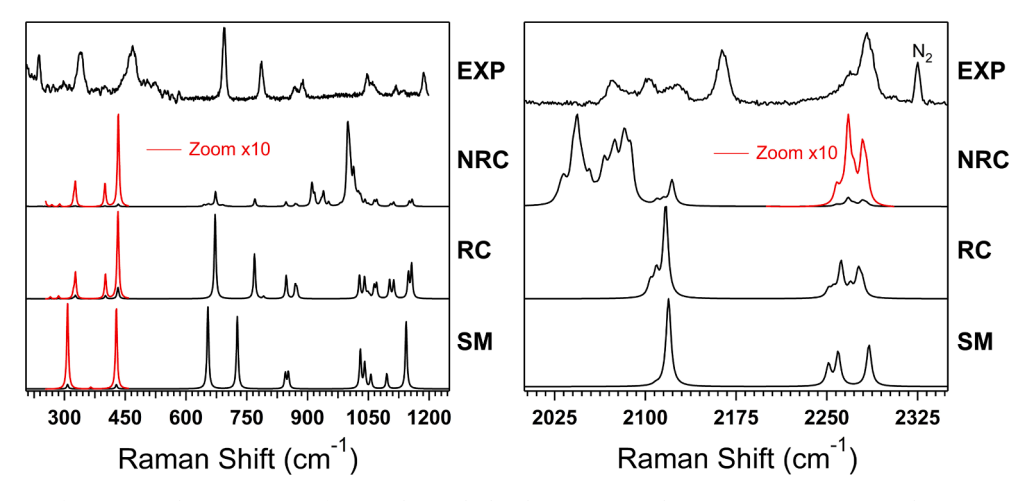


Fig. 6. Comparison of experimental RUNS spectra of TMAO-d<sub>9</sub> to calculated spectra using the P21/c space group using the RC, NRC, and SM models.

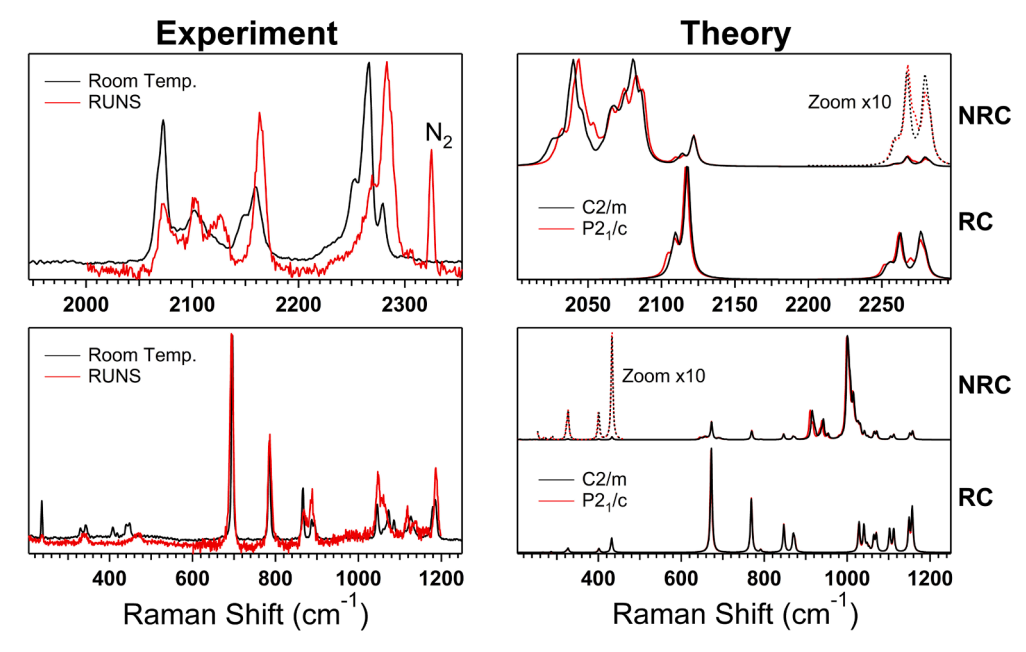


Fig. 7. Comparison of room temperature and RUNS spectra (left) and RC and NRC computational models using the C2/m and  $P2_1/c$  space groups (right) for TMAO-do.

GPa using a ruby F1 peak as a pressure reference.

As shown in Fig. 8a, continued compression of the all-hydrogen TMAO resulted in continuous blue shifts in all spectral regions. None of the observed modes demonstrated red shifts. The emergence of a shoulder peak can be seen in the 945 cm<sup>-1</sup> N-O stretch, where theory predicts the C-N stretch overlaps with the N-O stretch. While all of the modes in TMAO showed a similar degree of blue shifting, surprisingly, several of the modes in the TMAO-d<sub>9</sub> (Fig. 8b) showed very little deviations with increased pressure. In fact, the C-D wagging mode at 1124 cm<sup>-1</sup> exhibits no shifting within the resolution of the instrument. This result suggests that the interactions between neighboring TMAO-d9 molecules are not as significantly perturbed as the all hydrogen TMAO upon compression. At 5 GPa, the C-H stretching region shifts of around 30 cm<sup>-1</sup> were observed for TMAO which correspond to a roughly 1 percent increase in the energy of the mode; the C-D stretching region exhibited blue shifting less than 20 cm<sup>-1</sup> which is less than a 1 percent change in the mode's energy. The N-O stretch shows a similar degree of change between the two molecules while the C-N stretch is significantly more perturbed upon compression in TMAO-d<sub>9</sub>, blue shifting 35 cm<sup>-1</sup> (around 5%) compared to  $24 \text{ cm}^{-1}$  (around 3%) in TMAO.

#### 4. Conclusions

We have reported for the first time the crystal structures of perdeuterated TMAO at 220 K and 100 K and for TMAO at 100 K. Comparisons of TMAO and TMAO- $d_9$  Raman spectra revealed that even though the crystal structures are isomorphic, there are significant differences between the characteristic vibrational frequencies between the two systems and how these vibrational energies transform with increased pressure and decreased temperatures. TMAO- $d_9$  is significantly less perturbed than TMAO, which suggests weaker interactions between neighboring TMAO molecules. Even though the space group of the crystals changes at low temperatures, the effect on the vibrational structure is very limited. This is especially true for TMAO- $d_9$ , which exhibits only slight blue shifting of vibrational energies with increased pressure.

CRediT authorship contribution statement

**Louis E. McNamara:** Writing – original draft, Data curation, Conceptualization, Methodology. **Ethan C. Lambert:** Data curation,

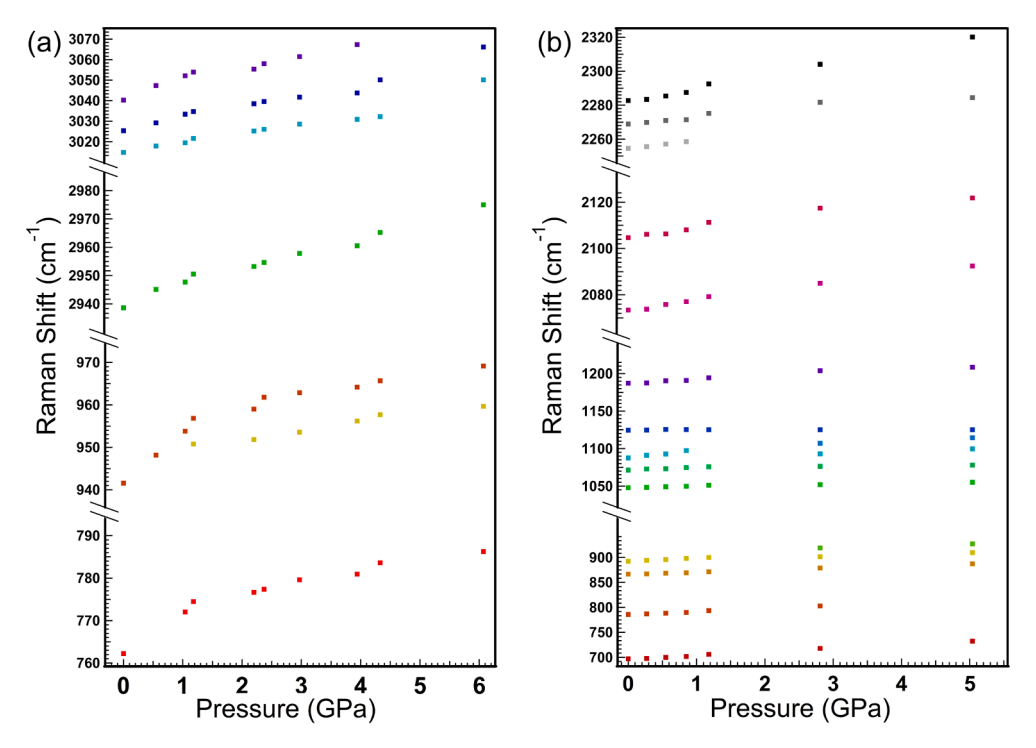


Fig. 8. Summary of frequency changes due to increased pressure of (a) TMAO and (b) TMAO-d<sub>9</sub>.

Investigation, Software, Writing - review & editing. Dana N. Reinemann: Writing - review & editing, Data curation, Conceptualization, Methodology. Henry Valle: Data curation. T. Keith Hollis: Supervision, Writing - review & editing. Gregory S. Tschumper: Data curation, Conceptualization, Methodology, Writing - review & editing, Supervision. Nathan I. Hammer: Supervision, Conceptualization, Methodology, Funding acquisition, Project administration, Writing - review & editing.

# **Declaration of Competing Interest**

The authors declare that they have no known competing financial interests or personal relationships that could have appeared to influence the work reported in this paper.

#### Data availability

Data will be made available on request.

#### Acknowledgement

This letter has been supported by the National Science Foundation under OIA-1757220 and CHE-1664998, as well as the Sally McDonnell Barksdale Honors College at the University of Mississippi. The computations in this letter were performed using resources at the Mississippi Center for Supercomputing Resources [MCSR].

### Author information

The manuscript was written through contributions of all authors. All authors have given approval to the final version of the manuscript. The authors declare that they have no known competing financial interests or personal relationships that could have appeared to influence the work reported in this paper.

# Appendix A. Supplementary data

Supplementary data to this article can be found online at https://doi.

org/10.1016/j.cplett.2022.139928.

#### References

- P.H. Yancey, M.E. Clark, S.C. Hand, R.D. Bowlus, G.N. Somero, Science 217 (1982) 1214–1222
- [2] D.R. Canchi, A.E. García, Annu. Rev. Phys. Chem. 64 (2013) 273-293.
- [3] S.S. Cho, G. Reddy, J.E. Straub, D. Thirumalai, J. Phys. Chem. B 115 (2011) 13401–13407.
- [4] Y. Zhang, P.S. Cremer, Annu. Rev. Phys. Chem. 61 (2010) 63-83.
- [5] D.W. Bolen, G.D. Rose, Annu. Rev. Biochem. 77 (2008) 339–362.
- [6] Q. Zou, B.J. Bennion, V. Daggett, K.P. Murphy, J. Am. Chem. Soc. 124 (2002) 1192–1202.
- [7] M.T. Record Jr, E.S. Courtenay, D.S. Cayley, H.J. Guttman, Trends Biochem. Sci. 23 (1998) 143–148.
- [8] P.H. Yancey, G.N. Somero, Biochem. J. 183 (1979) 317-323.
- [9] M. Auton, D.W. Bolen, Proc. Natl. Acad. Sci. 102 (2005) 15065-15068.
- [10] A. Wang, D.W. Bolen, Biochemistry 36 (1997) 9101–9108.
- [11] T.O. Street, D.W. Bolen, G.D. Rose, Proc. Natl. Acad. Sci. 103 (2006) 13997–14002.
- [12] S. Paul, G.N. Patey, J. Phys. Chem. B 111 (2007) 7932–7933.
- [13] A. Kuffel, J. Zielkiewicz, J. Chem Phy. 133 (2010), 035102.
- [14] P. Attri, P. Venkatesu, M.-J. Lee, J. Phys. Chem. B 114 (2010) 1471–1478.
- [15] V. Kocherbitov, V. Veryazov, O. Söderman, J. Mol. Struct. (Thoechem) 808 (2007) 111–118.
- [16] R.G.A.R. Maclagan, C. Malardier-Jugroot, M.A. Whitehead, M. Lever, J. Phys. Chem. A 108 (2004) 2514–2519.
- [17] K.M. Kast, J. Brickmann, S.M. Kast, R.S. Berry, J. Phys. Chem. A 107 (2003) 5342–5351.
- [18] K.M. Kast, S. Reiling, J. Brickmann, J. Mol. Struct. (Thoechem) 453 (1998) 169–180.
- [19] A.V.B. Yakimanskii, A. M.; Zubkov, V. A.; Petropavlovskii, G. A., Zh. Prikl. Khim., 64 (1991) 622–626.
- [20] N.G.B. Tsygankova, O. N.; Grinshpan, D. D.; Kaputskii, F. N., Vestsi Akad. Navuk BSSR, Ser. Khim. Navuk, (1988) 35–37.
- [21] R. Armstrong, M. Aroney, K. Calderbank, R. Pierens, Aust. J. Chem. 30 (1977) 1411–1415.
- [22] G.M. Phillips, J.S. Hunter, L.E. Sutton, J. Chem. Soc. (1945) 146–162.
- [23] E.P. Linton, J. Am. Chem. Soc. 62 (1940) 1945–1948.
- [24] K.A. Cuellar, K.L. Munroe, D.H. Magers, N.I. Hammer, J. Phys. Chem. B 118 (2013) 449–459.
- [25] A.Y. Rogachev, P. Burger, PCCP 14 (2012) 1985–2000.
- [26] P.M. Reddy, M. Taha, P. Venkatesu, A. Kumar, M.-J. Lee, J. Chem. Phys. 136 (2012) 234904.
- [27] J. Hunger, K.-J. Tielrooij, R. Buchner, M. Bonn, H.J. Bakker, J. Phys. Chem. B 116 (2012) 4783–4795.
- [28] G. Saladino, M. Marenchino, S. Pieraccini, R. Campos-Olivas, M. Sironi, F. L. Gervasio, J. Chem. Theory Comput. 7 (2011) 3846–3852.
- [29] K.L. Munroe, D.H. Magers, N.I. Hammer, J. Phys. Chem. B 115 (2011) 7699–7707.

- [30] G.A. Verville, M.H. Byrd, A. Kamischke, S.A. Smith, D.H. Magers, N.I. Hammer, J. Raman Spectrosc. 52 (2021) 788–795.
- [31] C.J. Sahle, M.A. Schroer, J. Niskanen, M. Elbers, C.M. Jeffries, C. Sternemann, PCCP 22 (2020) 11614–11624.
- [32] H.C. Urey, F.G. Brickwedde, G.M. Murphy, Phys. Rev. 39 (1932) 164-165.
- [33] G. Sheldrick, Acta Crystallogr. A 64 (2008) 112-122.
- [34] P. Hohenberg, W. Kohn, Phys. Rev. 136 (1964) B864–B871.
- [35] W. Kohn, L.J. Sham, Phys. Rev. 140 (1965) A1133-A1138.
- [36] M.J. Frisch, G.W. Trucks, H.B. Schlegel, G.E. Scuseria, M.A. Robb, J.R. Cheeseman, G. Scalmani, V. Barone, B. Mennucci, G.A. Petersson, H. Nakatsuji, M. Caricato, X. Li, H.P. Hratchian, A.F. Izmaylov, J. Bloino, G. Zheng, J.L. Sonnenberg, M. Hada, M. Ehara, K. Toyota, R. Fukuda, J. Hasegawa, M. Ishida, T. Nakajima, Y. Honda, O. Kitao, H. Nakai, T. Vreven, J.A. Montgomery Jr., J.E. Peralta, F. Ogliaro, M.J. Bearpark, J. Heyd, E.N. Brothers, K.N. Kudin, V.N. Staroverov, R. Kobayashi, J. Normand, K. Raghavachari, A.P. Rendell, J.C. Burant, S.S. Iyengar, J. Tomasi, M. Cossi, N. Rega, N.J. Millam, M. Klene, J.E. Knox, J.B. Cross, V. Bakken, C. Adamo, J. Jaramillo, R. Gomperts, R.E. Stratmann, O. Yazyev, A.J. Austin, R. Cammi, C. Pomelli, J.W. Ochterski, R.L. Martin, K. Morokuma, V.G. Zakrzewski, G.A. Voth, P. Salvador, J.J. Dannenberg, S. Dapprich, A.D. Daniels, Ö. Farkas, J.B. Foresman, J. V. Ortiz, J. Cioslowski, D.J. Fox, Gaussian 09, in, Gaussian, Inc., Wallingford, CT, USA, 2009.
- [37] A.D. Becke, J. Chem. Phys. 98 (1993) 5648-5652.
- [38] C. Lee, W. Yang, R.G. Parr, Phys. Rev. B 37 (1988) 785-789.
- [39] A.A. Howard, G.S. Tschumper, N.I. Hammer, J. Phys. Chem. A 114 (2010) 6803–6810.
- [40] S. Schlücker, J. Koster, R.K. Singh, B.P. Asthana, J. Phys. Chem. A 111 (2007) 5185–5191.
- [41] A.M. Wright, L.V. Joe, A.A. Howard, G.S. Tschumper, N.I. Hammer, Chem. Phys. Lett. 501 (2011) 319–323.
- [42] D.J. Scardino, A.A. Howard, M.D. McDowell, N.I. Hammer, J. Chem. Educ. 88 (2011) 1162–1165.
- [43] J.D. Barnett, S. Block, G.J. Piermarini, Rev. Sci. Instrum. 44 (1973) 1-9.
- [44] A. Jayaraman, Rev. Mod. Phys. 55 (1983) 65-108.
- [45] N.I.H. Robert N. Compton, Ethan C. Lambert, J. Stewart Hager, Raman Spectroscopy Under Liquid Nitrogen (RUN), Springer Cham, 2022.
- [46] J.S. Hager, J. Zahardis, R.M. Pagni, R.N. Compton, J. Li, J. Chem. Phys. 120 (2004) 2708–2718.
- [47] K.M. Dreux, L.E. McNamara, J.T. Kelly, A.M. Wright, N.I. Hammer, G. S. Tschumper, J. Phys. Chem. A 121 (2017) 5884–5893.
- [48] R.N. Compton, N.I. Hammer, J. Phys. Conf. Ser. 548 (2014), 012017.
- [49] A. Caron, G.J. Palenik, E. Goldish, J. Donohue, Acta Crystallogr. A 17 (1964) 102–108.